Relationship between the cochlear aqueduct and internal auditory canal: surgical implications for transcanal transpromontorial approaches to the lateral skull base

Giulia Molinari[1,2], MD; Abraam Yacoub[1,3,4], MD; Marco Bonali[2], MD; Wilhelm Wimmer[1,4], PhD; Matteo Alicandri-Ciufelli[2], MD, FEBORL-HNS; Marco Caversaccio[1,4], MD; Livio Presutti[2], MD; Lukas Anschuetz[1,4], MD

[1] Department of Otolaryngology Head and Neck Surgery, Inselspital, University Hospital and University of Bern, Switzerland

[2] Department of Otolaryngology Head and Neck Surgery, University Hospital of Modena, Italy

[3] Department of Otolaryngology Head and Neck Surgery, Faculty of Medicine, Ain Shams University, Cairo, Egypt

[4] Hearing Research Laboratory, ARTORG Center for Biomedical Engineering, University of Bern, Switzerland

Giulia Molinari and Abraam Yacoub contributed equally to this work.

Corresponding Author

Giulia Molinari, MD

Department of Otolaryngology Head and Neck Surgery, Inselspital, University Hospital and University of Bern, Freiburgstrasse 15, CH-3010 Bern, Switzerland

Email: dr.giuliamolinari@gmail.com, Tel: +41316322654; Fax: +41316324872

Conflicts of Interest: The authors disclose no conflict of interest.

Source of Funding: This study was partially funded by CTU-grant 2017-01 and matching grant by Karl Storz, Germany allocated to LA. The funders had no role in study design, data collection and analysis, decision to publish or preparation of the manuscript.

Abstract

Hypothesis: To investigate the anatomy of the cochlear aqueduct (CA) and its relationship with the internal auditory canal (IAC); to describe the surgical importance of the CA in minimally invasive approaches to the lateral skull base (LSB).

Background: Due to its close relationship to the lower cranial nerves and the jugular vein, the CA represents the inferior limit of dissection during transcanal transpromontorial approaches to the LSB.

Methods: Three-dimensional models from high-resolution computed tomography scans (HRCTs) of human temporal bones without pathology were created using threshold-based segmentation. All CA were classified into 4 categories. Five points were determined on the 3D models to measure the surgically relevant relationships.

Results: Segmentation was performed on 26 HRCTs**.** The average length of the virtual and visual part of the CA was 6.6 mm (SD ±1.7 mm) and 5.5 mm (SD ±1.3 mm) respectively. The mean distance between the IAC and the medial end of the visual part of the CA was 3.8 mm (±0.7 mm), while the average distance between the IAC and the lateral end was 1.4 mm (±0.6 mm). The distance between the visual part of the CA and the IAC increased by 0.25 mm per 1.0 mm from the fundus of the IAC.

Conclusion: The CA represents the inferior surgical limit of transpromontorial approaches to the LSB. The distance of the CA from the IAC could be described as a function of the position along the IAC and increases by 0.25 mm per each mm of the IAC from lateral to medial.

Introduction

The cochlear aqueduct (CA) is a narrow bony channel extending from the basal turn of the cochlea to the posterior cranial fossa (PCF). Its lumen, covered by fibroblastic cells and connective tissue, connects the perilymphatic space of the scala tympani to the subarachnoid space of the PCF, suggesting a role in fluid and pressure balance between the inner ear and cerebrospinal fluid (CSF).[1] The human CA anatomy has been investigated through histologic and radiologic investigations, and there seems to be great variability in shape, size, course and lumen patency. It remains unclear how anatomical features of the CA could possibly be related to pathologic conditions.[2-4] Regarding its normal shape, it is generally described as funnel-like[1]; some authors found it to have an hourglass shape[5], while a minority described dilation in its midportion.[6]

Recently, new endoscopic approaches to the internal auditory canal (IAC) and cerebellopontine angle (CPA) have been described. The exclusive endoscopic transcanal transpromontorial approach (EndoTTA) has been used since 2013 for the removal of small vestibular schwannomas (Koos stage I and II), through the external auditory canal.[7] Some technical and anatomical limitations of this approach were addressed by the expanded transcanal transpromontorial approach (ExpTTA), where endoscopic and microscopic techniques are combined.[8,9] These approaches allow direct access to the IAC from lateral to medial, with very little or no superficial tissue dissection and limited drilling of the petrous bone, compared to traditional approaches.[10] Therefore their application is increasingly spreading internationally. Given the limited area exposed using transcanal transpromontorial approaches[11], it is of utmost importance to identify anatomical landmarks enhancing the safety of these surgical techniques.

In understanding the surgical path to follow during transpromontorial approaches, it is significant to consider the CA as a pivotal anatomical structure, despite its variability.[12] In

fact, due to its close relationship to the lower cranial nerves (IX-XI), it represents the most inferior limit of dissection during transpromontorial surgery of the lateral skull base (Figure 1). The CA anatomy and its relationship to the IAC, with special consideration regarding the transpromontorial approaches, have not been investigated before. Therefore, we aim to investigate the anatomy of the human CA in relation to the IAC and describe its surgical importance in minimally invasive endoscopic lateral skull base surgery.

Material and Methods

Data acquisition

The present study was approved by our institutional review board (KEK-BE 2016-00887). High resolution computed tomography scans (HRCT) of adult temporal bones without pathology were acquired (SOMATOM Definition Edge, Siemens, Erlangen, Germany) with a voxel size of 0.156 x 0.156 x 0.2 mm^3.

Three-dimensional temporal bone reconstruction and measures

According to its visibility in HRCT, the CA was divided into a lateral virtual portion (not visible on HRCT), and a medial visual portion (visible in HRCT). According to the relationship between the virtual and visual parts of the CA on HRCT, all CA were classified, as previously proposed by Migirov et al., as: Type 1 - CA is visible in its entire course from the basal turn of the cochlea to the subarachnoid space, Type 2 - medial two-thirds of CA can be visualized, Type 3 - only the medial orifice or the medial one-third of CA is visible and Type 4 - corresponding to CA not detectable at all.[13]

From the HRCT data, three-dimensional (3D) surface models of the temporal bone were created using threshold-based segmentation (Amira, FEI, France). Each specimen underwent manual segmentation of the following structures: facial nerve, bony labyrinth, internal carotid artery, jugular bulb, IAC, and visual portion of the CA (Figure 2A).

The 3D models were subsequently used to measure the surgically relevant topographical relationships. Therefore, 5 points were determined on the reconstructed 3D models, as illustrated in Figure 2B: (1) medial lower limit of the IAC, (2) lateral lower limit of the IAC, (3) medial end of the visual part of the CA (corresponding to the opening of the CA into the posterior cranial fossa), (4) lateral end of the visual part of the CA and (5) virtual opening of the CA into the medial end of the round window. Through the connection of these 5 points, two lines were obtained: the upper, between points 1 and 2, represents the lower border of the IAC, and the lower, between point 3 to 5 results in an angled line representing the course of the CA. Distance calculations were performed with a MATLAB script (The MathWorks Inc., Natick, MA). The Cartesian coordinates of the above mentioned 5 points were imported. The landmarks indicating the CA were used to compute a reference plane for each specimen. Then, the normal distances of the IAC landmarks with respect to the plane were calculated. The datasets analysed during the study are available from the corresponding author on reasonable request.

Results

A total of 30 HRCTs of adult temporal bones without evident pathology were acquired. Four (4/30, 13%) were excluded from segmentation process, as they presented type 4 CA (not detectable). Among those suitable for segmentation, 3 were type 1(3/30, 10%), 21 type 2 (21/30, 70%), and 2 type 3 (2/30, 7%). Examples of segmented models for each type of CA are illustrated in Figure 3.

The average length of the virtual part of the CA measured 6.6 mm (SD ±1.7 mm) and the average length of the visual part was 5.5 mm (SD ±1.3 mm) as illustrated in Figure 4. The mean length of the IAC was 7.9 mm (±1.1 mm).

To describe the surgical importance of the CA during transpromontorial approaches to the IAC, the vertical distance between the CA and the lower limit of the IAC was measured

and was found to increase from lateral to medial. The mean distance between the IAC and the medial end of the visual part of the CA was 3.8 mm (±0.7 mm), while the average distance between the IAC and the lateral end of the visual part was 1.4 mm (±0.6 mm), as illustrated in Figure 5. This topographical relationship between the mean distance of the IAC and the visual part of the CA is described as a function of the position along the IAC (emerging from lateral to medial) in Figure 6. On average, the distance between the visual part of the CA and the IAC increased by 0.25 mm per 1.0 mm distance from the most lateral point of the IAC (corresponding to the fundus). We did not observe statistically significant correlations between the lengths of the visual and virtual parts of the CA and the distance to the IAC.

Discussion

This study investigates the surgical relevance of the CA during minimally invasive endoscopic lateral skull base surgery. A correlation between the distances of the CA to the IAC and the distance from the fundus of the IAC is described.

Following the surgical corridor of the transpromontorial approaches, the CA is found close to the lateral part of the IAC, as it emerges from the basal turn of the cochlea. As the dissection proceeds towards the IAC porus, the CA gradually moves away from the IAC in an infero-medial direction, with an increasing distance of 0.25 mm per 1.0 mm from the most lateral point of the IAC. Despite the rather low number of investigated temporal bones, the standard deviation is less than 1.0 mm (lateral 0.6 mm and medial 0.7 mm) and therefore the provided measurements may be considered reliable in identifying the inferior limit of dissection during minimally invasive surgery of the lateral skull base.

As recently described by Atturo et al, the CA is paralleled in its course by up to three bony channels named accessory channels (AC).[14] The first AC (AC1) is described as constant and housing the inferior cochlear vein (ICV), which drains most of the cochlear blood flow.

This canal, also known as Cotugno's canal, was already described by Gopec and Jackler, as a separate bony channel that started just cranial to the cochlear end of the aqueduct and continued antero-inferiorly close to the CA, until the vein drained into the inferior petrosal sinus or into the jugular bulb.[1,15] The importance of this collateral vein is illustrated in Figure 7 (A and B), showing intraoperative images of an ExpTTA for vestibular schwannoma removal: the CA can be indirectly identified by the bleeding from the inferior cochlear vein and its collaterals, if its lumen is surgically not visible. This bleeding could be easily managed by the application of resorbable hemostatic agents, adrenaline-soaked cottonoids or bone wax. Drilling of this region with a diamond burr ensures further bleeding control and allows exposing the IAC, which is located just medially.

Moreover, it is suggested that the second AC (AC2) carries a collateral vein draining the floor of the middle ear directly to the jugular foramen, representing a direct connection between the middle ear and the intracranial veins, through which infectious processes could expand and lead to thrombosis of the venous intracranial sinuses. Anastomoses and interactions with AC1 were found.[14] CA has been proposed indeed as a possible route of intracranial extent of infections deriving from the middle ear and mastoid.[13,16] Given the proximity of the ICV to electrode trajectory sites in cochlear implant surgical procedures, it has been speculated about the importance of the ICV in hearing preservation. An accidental section or obstruction of the ICV during surgery could impair the function of ganglion cells and therefore lead to hearing loss.[14] This consideration is especially important for other applications of minimally invasive endoscopic lateral skull base surgery as, for example, the transcanal infracochlear approach to the inferior petrous apex, where the preservation of the venous drainage of the cochlea may be crucial for favorable results regarding hearing preservation.

Despite the variability in its shape and course, the structure of the CA could be overall divided into four portions, from lateral to medial: 1. cochlear opening; 2. lateral otic capsule

segment; 3. medial petrous apex portion; 4. cranial opening.[1,15] The cochlear opening, located in the scala tympani of the basal turn of the cochlea, forms the so-called cochlear aqueduct-round window membrane complex.[17] Running through the otic capsule, the CA reaches its narrowest diameter[13]; then it continues with the petrous apex portion, which is typically wider and subject to greater variability. The cranial orifice of the CA opens medially in the inferior surface of the petrous bone, between the IAC and the anterior division of the jugular foramen, close to the glossopharyngeal nerve.[1,16,17]

This anatomical relationship has significant surgical implications as a transpromontorial approach to the IAC performed below the level of the CA may expose the lower cranial nerves and the jugular vein, thereby risking injury to these structures. The proximity of the IAC to the jugular foramen also implies that a high riding jugular bulb may constitute a relative contraindication to transpromontorial approaches, since the inferior limit of the surgical dissection would be restricted by the presence of the vein.

In contrast to the vestibular aqueduct, which hosts the endolymphatic duct within, several anatomists have reported that the CA does not have a lumen *per se*, rather is filled with a meshwork of loose connective tissue. As reported by Gopen et al, the patency of the CA could be classified into four categories, according to histologic evaluation: patent lumen, defined as presence of a lumen throughout the entire length of the aqueduct; lumen filled with loose connective tissue, defined as lumen occupied by connective tissue in at least one section; lumen occluded by bone, when the lumen is completely filled with a bony plug separated from the CA itself, in at least one section; obliteration of the aqueduct, defined as a missing or absent aqueduct in part or all of its course.[1] It is not clear the role age could play in modifying the patency or width of the lumen.[18]

Considering the variability of the CA anatomy, its small size, and the cases of obliterated or radiologic type 4 CA, its intraoperative identification might be quite challenging. In these cases the identification of the CA during transpromontorial approaches is usually possible

due to the bleeding of the accessory veins parallel to its course. If available, the use of image-guided neuronavigation ideally with an accuracy in the submillimeter scale, is advocated for patients undergoing minimally invasive approaches to the lateral skull base.[19,20]

The anatomical relationship between the CA and the IAC has been investigated for the first time, underlining that the CA plays a crucial role as the most inferior limit of dissection during transcanal transpromontorial approaches to the lateral skull base. Our results might suggest that the CA should be thoroughly evaluated in preoperative HRCT of the temporal bone before minimally invasive approaches to the IAC and CPA, as the course and visibility of this structure exhibit some range of variability. Type 4 CA may represent a limitation of the application of CA as a dissection boundary; however, the incidence of this radiologic category is overall low (13% in this study). Also, given the possibility to indirectly assess CA position intraoperatively by collateral veins bleeding, this issue should not impede with the suitability of the CA as a landmark during transpromontorial approaches.

Despite the limited number of specimens included in the study, the provided measurements could be considered highly reliable as performed on 3D models derived from the segmentation of clinical human temporal bone HRCTs. The standard deviation of the mean distances between the IAC and the lateral and medial end of the visual CA respectively is negligible, thus the function describing the relation of the two anatomical structures should be considered acceptable.

In conclusion, the distance of the CA from the IAC could be described as a function of the distance from the fundus of the IAC and increases by 0.25mm per 1.0mm inside the IAC, from lateral to medial. Understanding the surgical implications of this relationship is essential to perform safe minimally invasive lateral skull base surgery, avoiding damage to the lower cranial nerves, as well as the jugular vein.

References

1. Gopen Q, Rosowski JJ, Merchant SN. Anatomy of the normal human cochlear aqueduct with functional implications. *Hear Res* 1997;107:9-22.
2. Stimmer H. Enlargement of the cochlear aqueduct: Does it exist? *Eur Arch Otorhinolaryngol* 2011;268:1655-61.
3. Song C Il, Kang WS, Lee JH et al. Diameter of the medial side of the cochlear aqueduct is narrower in Meniere's disease: A radiologic analysis. *J Int Adv Otol* 2016;12:156-60.
4. Park JJH, Shen A, Keil S et al. Radiological findings of the cochlear aqueduct in patients with Meniere's disease using high-resolution CT and high-resolution MRI. *Eur Arch Otorhinolaryngol* 2014;271:3325-31.
5. Ritter FN, Lawrence M. A histological and experimental study of cochlear aqueduct patency in the adult human. *Laryngoscope*1965;75:1224-33.
6. Kelemen G, La Fuente DA, Perez Olivares F. The cochlear aqueduct: structural considerations. *Laryngoscope* 1979;89:639-45
7. Marchioni D, Alicandri-Ciufelli M, Rubini A et al. Exclusive endoscopic transcanal transpromontorial approach: a new perspective for internal auditory canal vestibular schwannoma treatment. *J Neurosurg* 2016;126:98-105.
8. Presutti L, Bonali M, Marchioni D et al. Expanded transcanal transpromontorial approach to the internal auditory canal and cerebellopontine angle : a cadaveric study. *Acta Otorhinolaryngol Ital* 2017;37:224-30.
9. Presutti L, Alicandri-Ciufelli M, Bonali M et al. Expanded transcanal transpromontorial approach to the internal auditory canal: Pilot clinical experience. *Laryngoscope* 2017;127:2608-14.
10. Alicandri-Ciufelli M, Federici G, Anschuetz L et al. Transcanal surgery for vestibular schwannomas: a pictorial review of radiological findings, surgical anatomy and

comparison to the traditional translabyrinthine approach. *Eur Arch Otorhinolaryngol* 2017;274:3295-02.

11. Anschuetz L, Presutti L, Schneider D et al. Quantitative Analysis of Surgical Freedom and Area of Exposure in Minimal-Invasive Transcanal Approaches to the Lateral Skull Base. *Otol Neurotol* 2018;39:785-90.
12. Li Z, Shi D, Li H et al. Micro-CT study of the human cochlear aqueduct. *Surg Radiol Anat* 2018;40:713-20.
13. Migirov L, Kronenberg J. Radiology of the cochlear aqueduct. *Ann Otol Rhinol Laryngol* 2005;114(11):863-66.
14. Atturo F, Schart-Morén N, Larsson S et al. The human cochlear aqueduct and accessory canals : a micro-CT analysis using a 3D reconstruction paradigm. *Otol Neurotol* 2018; 39:e429-e435.
15. Jackler RK, Hwang PH. Enlargement of the cochlear aqueduct: Fact or fiction? *Otolaryngol Head Neck Surg* 1993;109:14-25.
16. Arnold W, Bredberg W, Gstottner W et al. Meningitis following cochlear implantation: pathomechanisms, clinical symptoms, conservative and surgical treatments. *ORL J Otorhinolaryngol Relat Spec* 2002;64:382-89.
17. Hofman R, Segenhout JM, Albers FWJ et al. The relationship of the round window membrane to the cochlear aqueduct shown in three-dimensional imaging. *Hear Res* 2005;209:19-23.
18. Włodyka J. Studies on cochlear aqueduct patency. *Ann Otol Rhinol Laryngol* 1978;87:22-28.
19. Rathgeb C, Anschuetz L, Schneider D et al. Accuracy and feasibility of a dedicated image guidance solution for endoscopic lateral skull base surgery. *Eur Arch Otorhinolaryngol* 2018;275:905-11.
20. Schneider D, Hermann J, Gerber KA, et al. Noninvasive registration strategies and

advanced image guidance technology for submillimeter surgical navigation accuracy in the lateral skull base. *Otol Neurotol* 2018;39:1326-35.

Figure legends

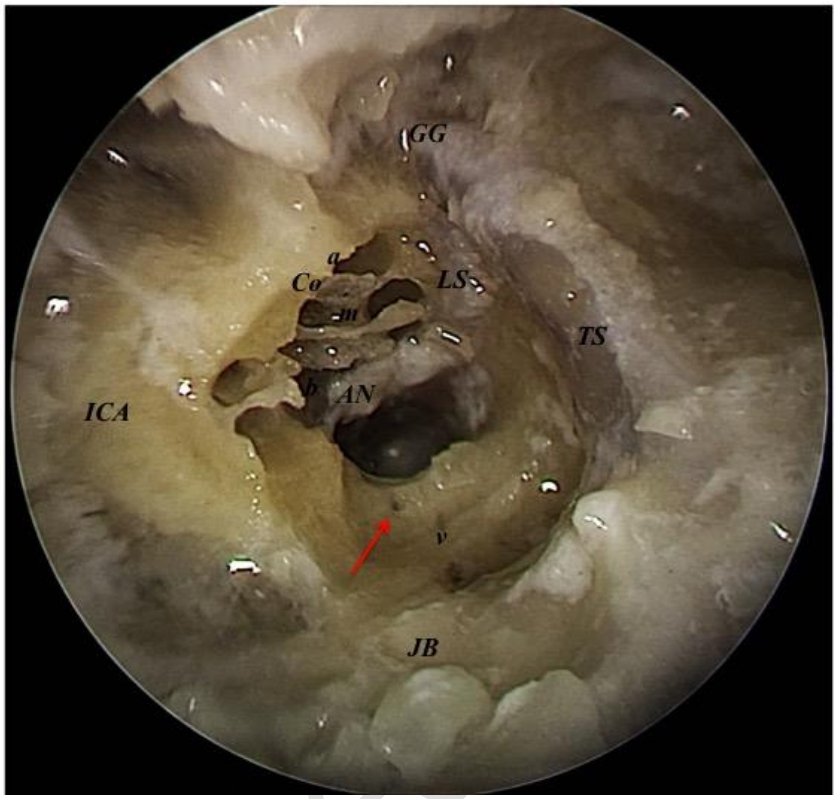

Fig 1. View of the cochlear aqueduct (red arrow) during endoscopic transcanal transpromontorial dissection in a human cadaver (left side). The bone removal towards the IAC should not proceed more caudally than this level. *v*, accessory vein to CA*; JB*, jugular bulb area; *ICA*, internal carotid artery area, *Co*, opened cochlea; *a*, apex of the cochlea; *m*, modiolus; *b*, basal turn of the cochlea; AN, acoustic nerve; *GG*, geniculate ganglion*; LS:* labyrinthine segment of the facial nerve*; TS:* tympanic segment of the facial nerve.

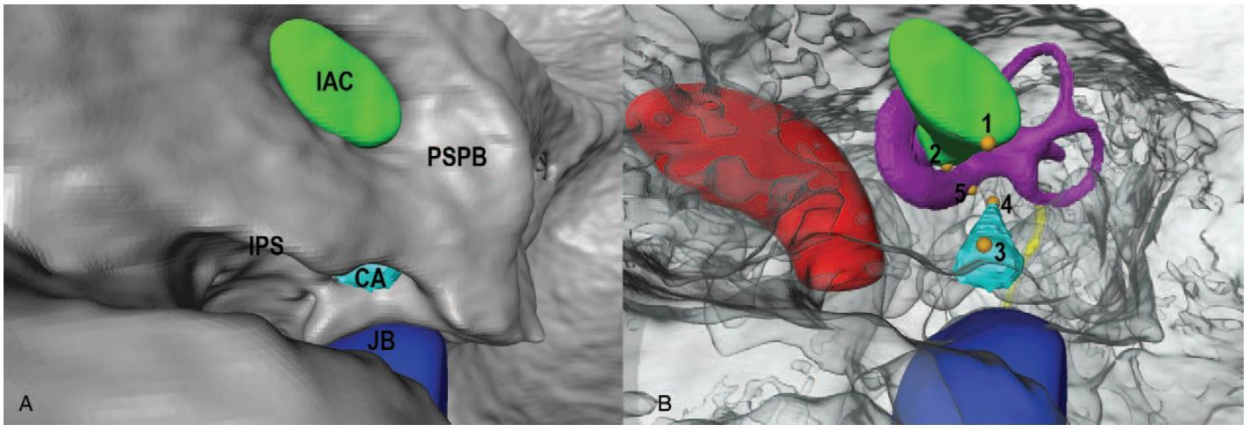

Fig 2. A 3D model based on segmentation from temporal bone HRCT (right side). Green: internal auditory canal (IAC); light blue: cochlear aqueduct (CA); purple: bony labyrinth; yellow: facial nerve; red: internal carotid artery; blue: jugular bulb. Star guide – S: superior; I: inferior; A: anterior; P: posterior. Figure A: Surgical perspective. Figure B: Medial-to-lateral perspective; 1: medial lower limit of the IAC; 2: lateral lower limit of the IAC; 3: medial end of the visual part of the CA; 4: lateral end of the visual part of the CA; 5: virtual opening of the CA into the round window.

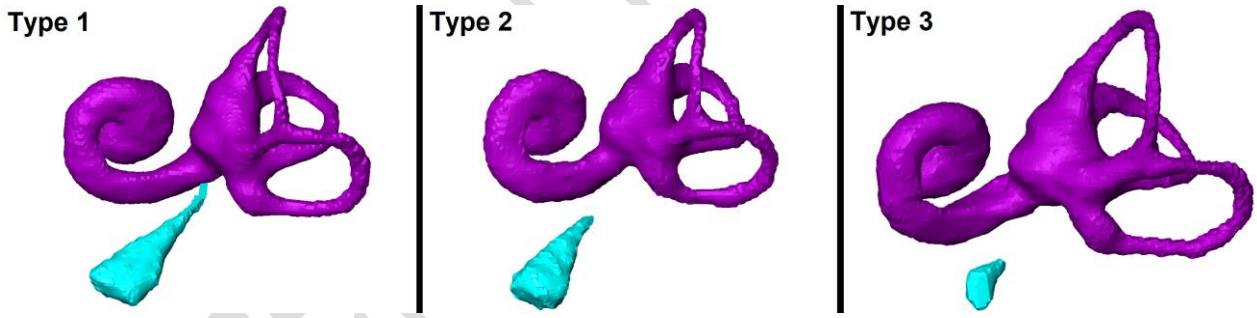

Fig 3. 3D models of three different categories of cochlear aqueduct (light blue) according to radiologic classification and relationship to the bony labyrinth (purple).

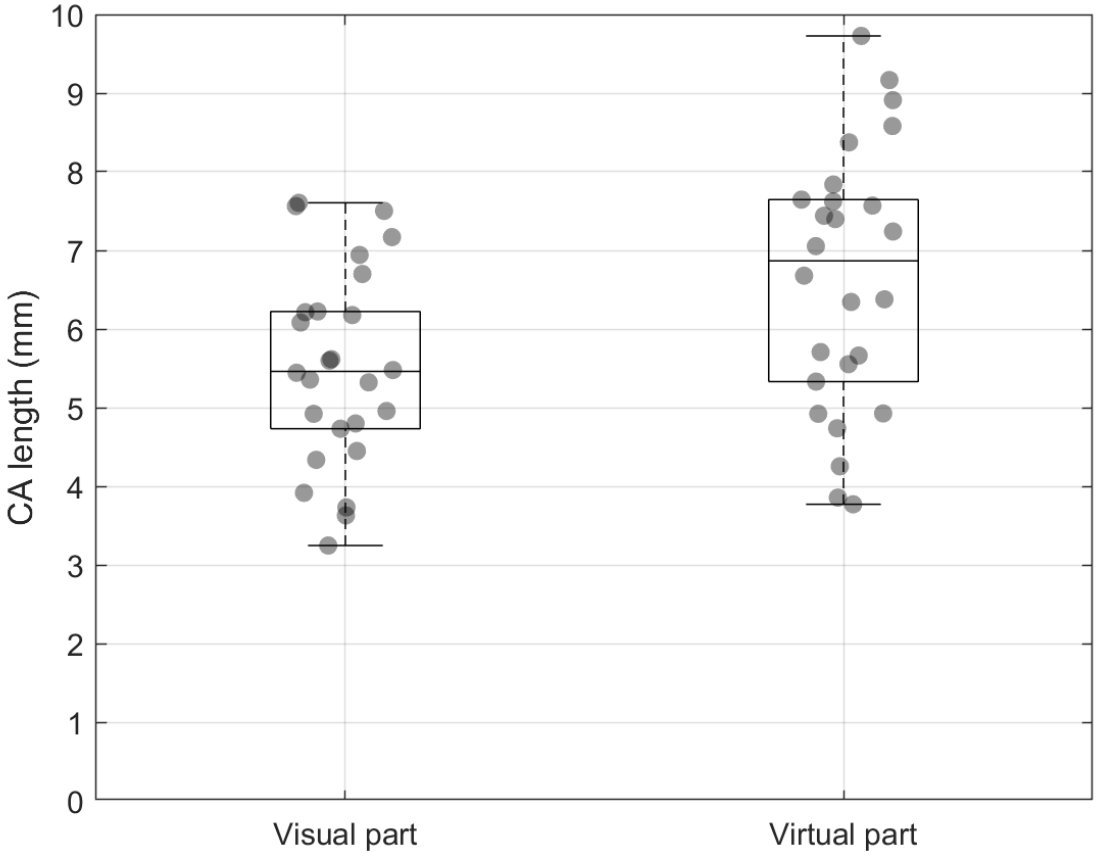

Fig 4. Box plot showing the average length of the visual and virtual part of the cochlear aqueduct respectively.

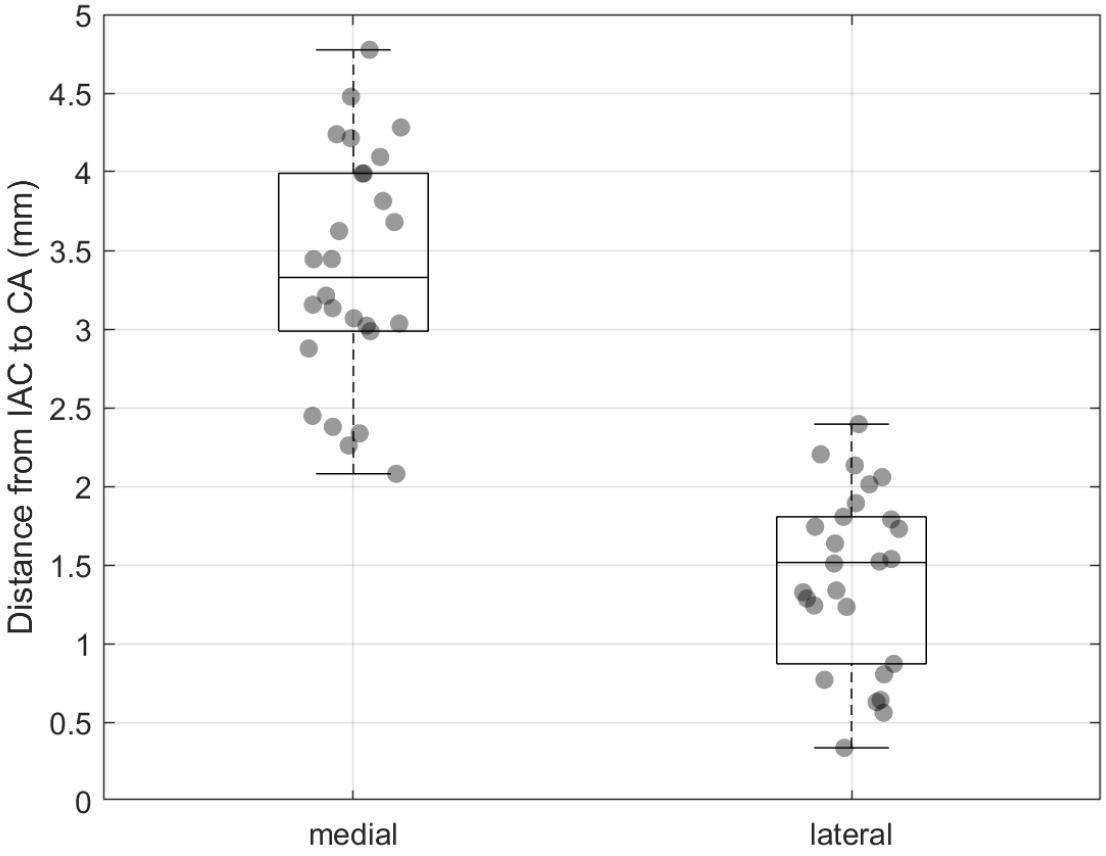

Fig 5. Box plot showing the mean distance between the internal auditory canal and the lateral and medial end of the visual part of the cochlear aqueduct respectively.

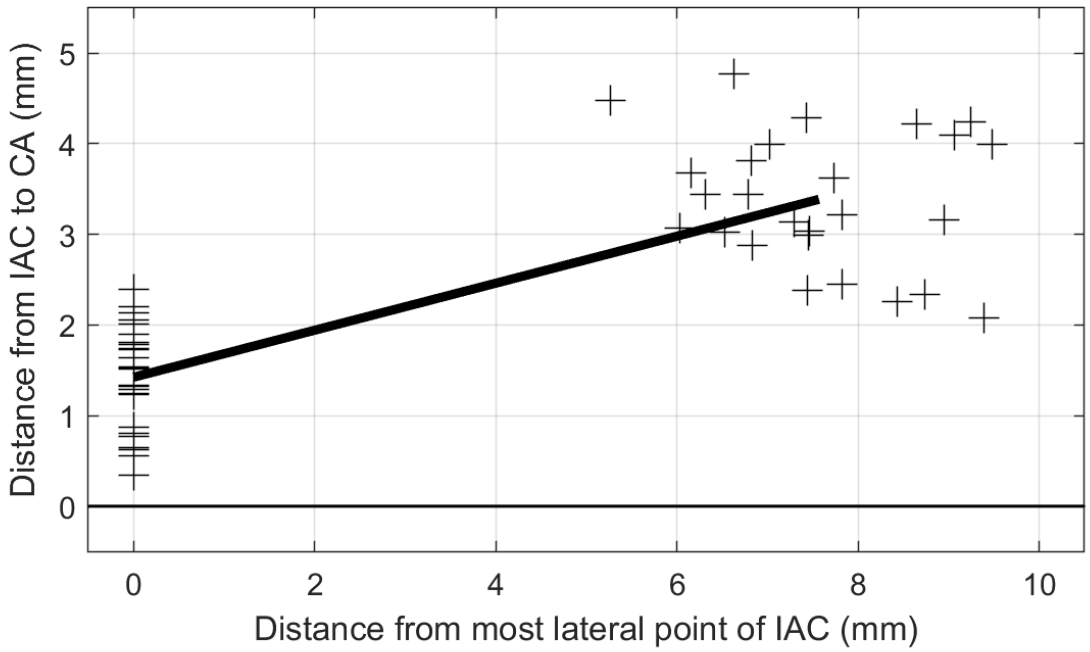

Fig 6. The mean distance between the internal auditory canal (IAC) and the visual part of the cochlear aqueduct as a function of the distance from the fundus of IAC.

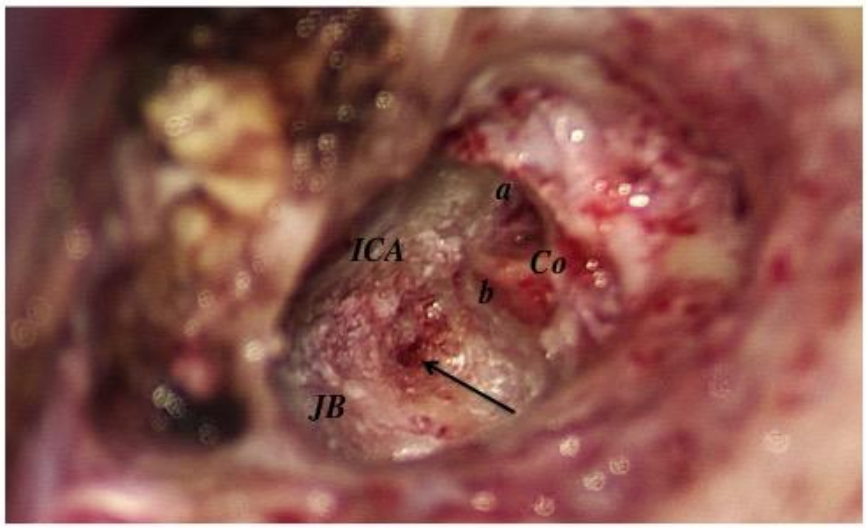

Fig 7. Exposure of the cochlear aqueduct (CA) during expanded transcanal transpromontorial approach for vestibular schwannoma removal (left side), microscopic view. Figure A: CA lumen, indicated by the arrow. *JB*, jubular bulb; *ICA*, internal carotid artery, *Co*, opened cochlea; *a*, apex of the cochlea; *b*, basal turn of the cochlea. Figure B: Bleeding from the inferior cochlear vein and collateral veins, from the CA region.